

Introduction to Numerical Hydrodynamics and Radiative Transfer

Part II: Hydrodynamics, Lecture 3

HT 2012

Susanne Höfner
Susanne.Hoefner@physics.uu.se

Introduction to Numerical Hydrodynamics

2. The Linear Advection Equation



2.3 Basic Concepts and Tools ... continued

Discretization in Space: Concepts

Representation of the “real” distribution of a variable by a finite set of numbers (on a spatial grid)

Restriction:

transformation from continuous values to discrete representation

Reconstruction:

transformation from discrete representation to continuous values

Finite difference methods:

- restriction: sampling, e.g.: $\rho_i = \rho(x_i)$
- reconstruction: interpolation (polynomials)
- derivatives become finite differences

Discretization in Space: Concepts

Representation of the “real” distribution of a variable by a finite set of numbers (on a spatial grid)

Restriction:

transformation from continuous values to discrete representation

Reconstruction:

transformation from discrete representation to continuous values

Finite volume methods:

- restriction: integration over control volume, e.g.:

$$\rho_i = \frac{1}{\Delta x} \int_{x_i - \Delta x/2}^{x_i + \Delta x/2} \rho(x) dx .$$

- reconstruction: by polynomials
- derivatives can become finite differences, or can be avoided

Discretization in Space: Concepts

Finite element methods:

- Representation by a finite set of simple base functions (piecewise polynomials) with compact ("finite") support
- Usually used on an unstructured grid to model the flow around complex bodies
- More often used in engineering than in astrophysics

Spectral methods:

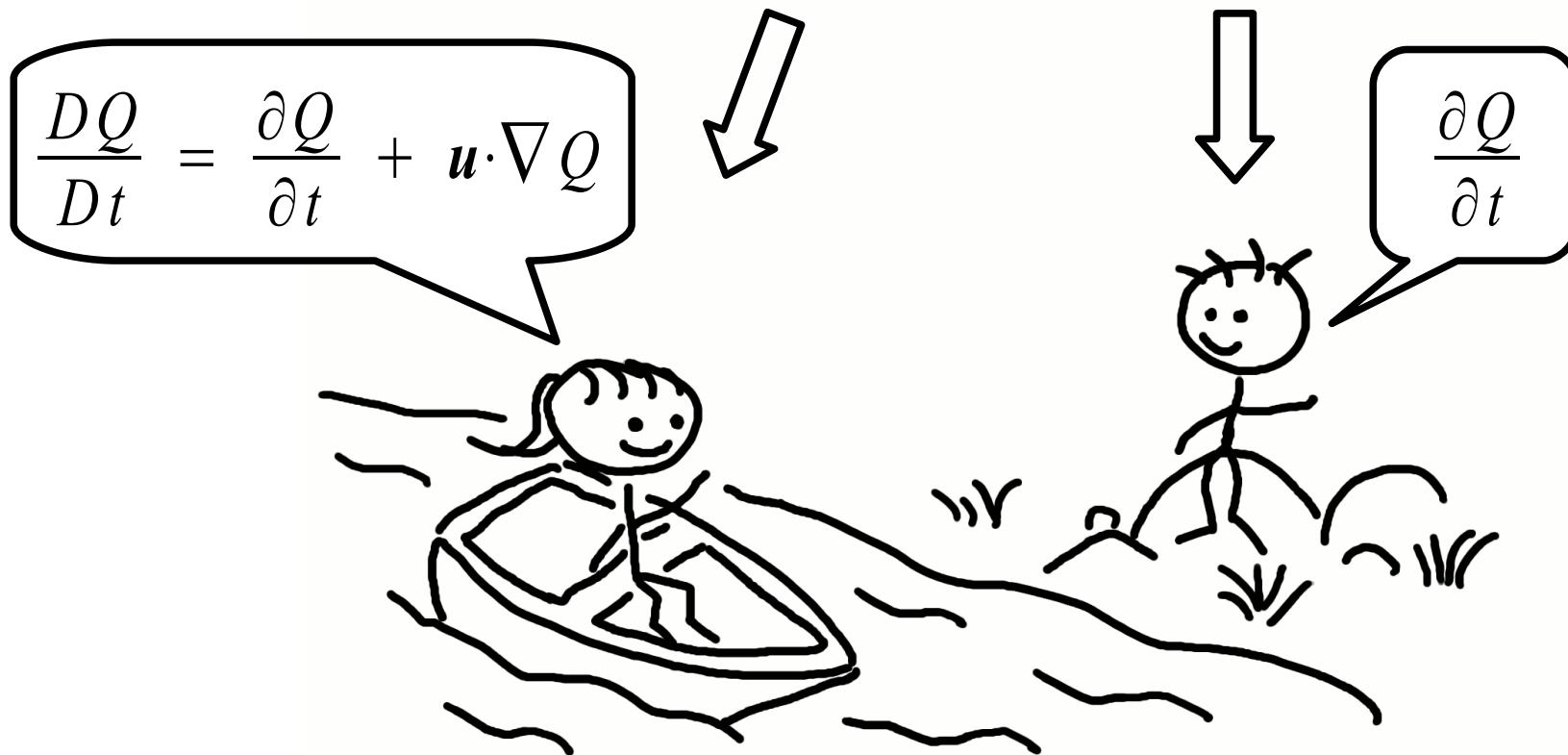
- Representation by a finite set of harmonical functions (e.g. sine waves)
- Spatial derivatives become multiplications with wavevector
- Good for flows with small non-linear interactions
- Typically used for flows in the stellar interior (with low Mach numbers)

Smoothed Particle Hydrodynamics (SPH):

- Representation by a finite set of "large particles" that move freely
- Grid is replaced by particle positions
- Particle density translates into fluid density

Discretization in Space: Concepts

Frame of reference: Lagrangian vs. Eulerian grids



Integral Form and Weak Solution

Any solution of the advection equation in differential form involves derivatives.

However, any function – even a discontinuous one – can be propagated along characteristics (see, e.g., Homework 1).

In certain cases, it may be important to avoid derivatives and/or discontinuities.

Transformation: linear advection equation in **integral form**:

$$\int_{x_0}^{x_1} [\rho(x, t_1) - \rho(x, t_0)] dx + v \int_{t_0}^{t_1} [\rho(x_1, t) - \rho(x_0, t)] dt = 0$$

Definition: Solution of the PDE in integral form \leftrightarrow **weak solution** of the PDE in differential form.

In smooth regions: weak solution = solution.

Integral Form and Flux Centering

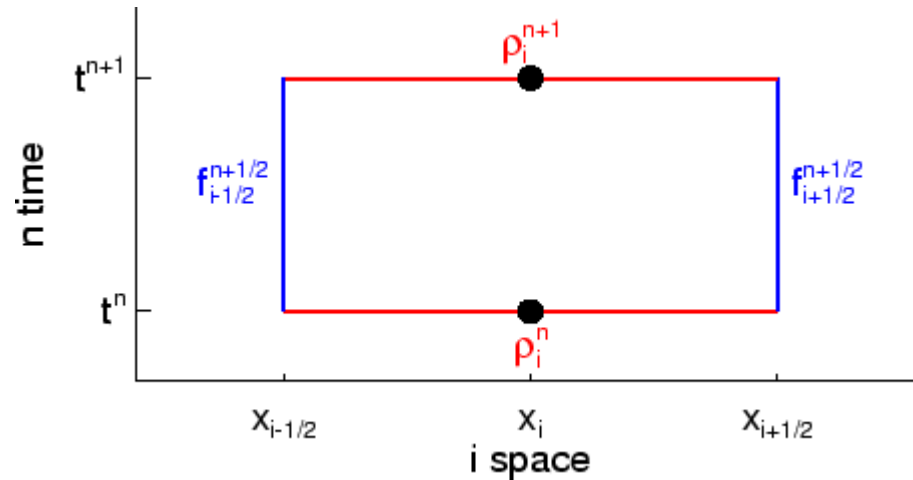


Figure courtesy of Bernd Freytag

Transformation: linear advection equation in **integral form**:

$$\int_{x_0}^{x_1} [\rho(x, t_1) - \rho(x, t_0)] dx + v \int_{t_0}^{t_1} [\rho(x_1, t) - \rho(x_0, t)] dt = 0$$

... for one grid cell and one time step:

$$\underbrace{\int_{x_{i-\frac{1}{2}}}^{x_{i+\frac{1}{2}}} \rho(x, t^{n+1}) dx}_{\Delta x \rho_i^{n+1}} - \underbrace{\int_{x_{i-\frac{1}{2}}}^{x_{i+\frac{1}{2}}} \rho(x, t^n) dx}_{\Delta x \rho_i^n} + \underbrace{\int_{t^n}^{t^{n+1}} v \rho\left(x_{i+\frac{1}{2}}, t\right) dt}_{\Delta t f_{i+\frac{1}{2}}^{n+\frac{1}{2}}} - \underbrace{\int_{t^n}^{t^{n+1}} v \rho\left(x_{i-\frac{1}{2}}, t\right) dt}_{\Delta t f_{i-\frac{1}{2}}^{n+\frac{1}{2}}} = 0$$

Centering of Quantities, Fluxes, and Differences

Examples for “natural centering”:

- quantities at grid points (integer i indices), e.g.: $\rho_i^n, \rho_{i+1}^n, \dots$
- spatial differences (half-integer i indices), e.g.: $\Delta\rho_{i+\frac{1}{2}}^n = \rho_{i+1}^n - \rho_i^n$
- time differences (half-integer n indices), e.g.: $\Delta\rho_i^{n+\frac{1}{2}} = \rho_i^{n+1} - \rho_i^n$
- fluxes at half-integer i indices (and, in fact, preferably at half-integer n indices) to get update properly centered:

$$\Delta\rho_i^{n+\frac{1}{2}} = -\frac{\Delta t}{\Delta x} \left(f_{i+\frac{1}{2}}^n - f_{i-\frac{1}{2}}^n \right)$$

Effects of “natural centering”:

$$\frac{\rho_{i+1}^n - \rho_i^n}{x_{i+1} - x_i} \text{ is } O(\Delta x) \text{ for } \frac{\partial \rho}{\partial x}(x_i) \text{ and } \frac{\partial \rho}{\partial x}(x_{i+1})$$
$$O(\Delta x^2) \text{ for } \frac{\partial \rho}{\partial x}\left(x_{i+\frac{1}{2}}\right)$$

$$\frac{\rho_{i+1}^n - \rho_{i-1}^n}{x_{i+1} - x_{i-1}} \text{ is } O(\Delta x^2) \text{ for } \frac{\partial \rho}{\partial x}(x_i)$$

Update Formula in Conservation Form

After computing the fluxes at the cell boundaries $f_{i+\frac{1}{2}}^n$ that characterize a method

(e.g. from the fluxes in the cells: $f(\rho_i^n) = v \rho_i^n$)

the update can be done by the formula

$$\rho_i^{n+1} = \rho_i^n - \frac{\Delta t}{\Delta x} \left(f_{i+\frac{1}{2}}^n - f_{i-\frac{1}{2}}^n \right) .$$

This is the **conservation form** because the density changes only due to fluxes through the boundaries, and is conserved otherwise:

$$\begin{aligned} \sum_{i=i_0}^{i_1} \rho_i^{n+1} &= \sum_{i=i_0}^{i_1} \rho_i^n + \frac{\Delta t}{\Delta x} \sum_{i=i_0}^{i_1} \left(f_{i+\frac{1}{2}}^n - f_{i-\frac{1}{2}}^n \right) \\ &= \sum_{i=i_0}^{i_1} \rho_i^n + \frac{\Delta t}{\Delta x} \left[f_{i_1+\frac{1}{2}}^n + \sum_{i=i_0}^{i_1-1} \left(f_{i+\frac{1}{2}}^n - f_{i+\frac{1}{2}}^n \right) - f_{i_0-\frac{1}{2}}^n \right] \\ &= \sum_{i=i_0}^{i_1} \rho_i^n + \frac{\Delta t}{\Delta x} \left(f_{i_1+\frac{1}{2}}^n - f_{i_0-\frac{1}{2}}^n \right) . \end{aligned}$$

Stencil Diagrams

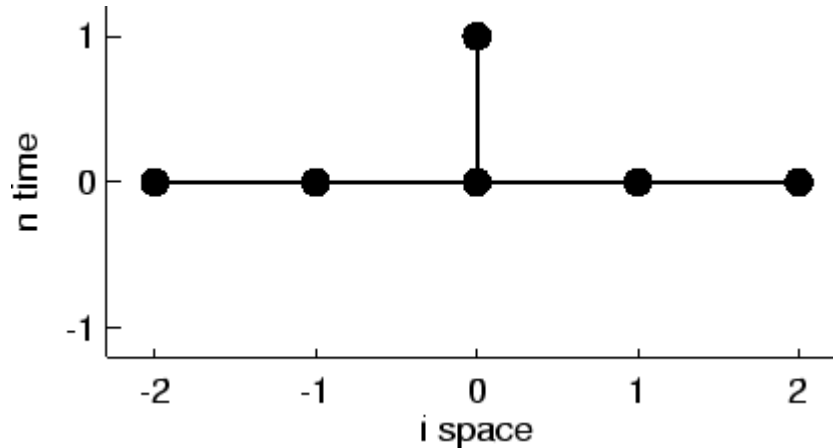


Figure courtesy of Bernd Freytag

The density ρ_i^{n+1} at grid point i and time step $n+1$ depends on values at the old time step n (direct **numerical domain of dependence, stencil**)

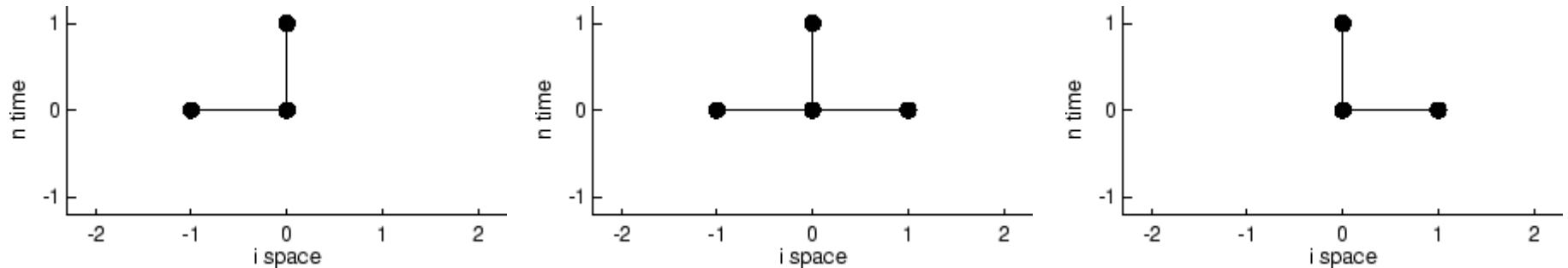
$$\rho_{i-k}^n, \rho_{i-k+1}^n, \dots, \rho_{i+l}^n \cdot$$

This is sketched in a so-called **stencil diagram**. On the other hand, the diagram shows also which points

$$\rho_{i-l}^{n+1}, \rho_{i-l+1}^{n+1}, \dots, \rho_{i+k}^{n+1}$$

at the new time step $n+1$ are influenced by ρ_i^n (**range of influence**).

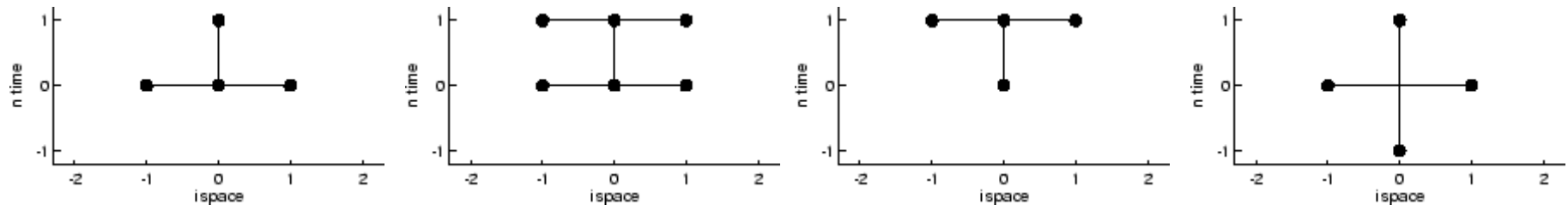
Stencil Diagrams: Spatial Centering



The figure above shows stencil diagrams for 3 schemes with FT (forward-time) centering and different spatial centerings:

- **BS**: backward-space (FTBS, left)
- **CS**: center-space (FTCS, middle)
- **FS**: forward-space (FTFS, right)

Stencil Diagrams: Centering in Time



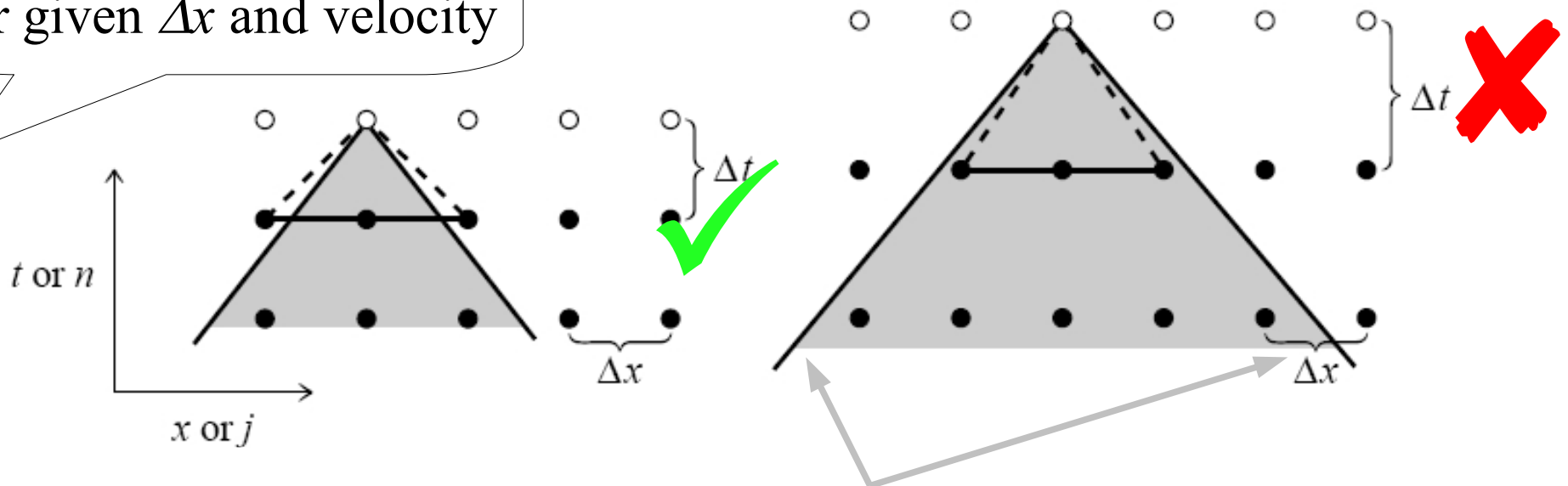
The figure above shows stencil diagrams for 4 schemes with CS (center-space) and different time centerings:

- **FT**: forward-time (explicit)
- **time-centered implicit** (implicit)
- **BT**: backward-time (fully implicit)
- **CT, Leapfrog**: center-time (explicit, uses 3 time planes)

In **implicit schemes** each value at the new time level typically depends on all values at the old level: The full domain of dependence is larger than the direct domain of dependence.

Domain of Dependence and CFL Condition

CFL condition **limits Δt**
for given Δx and velocity



Hyperbolic PDEs have a finite physical domain of dependence due to the finite travelling speed of waves (\leftrightarrow characteristics).

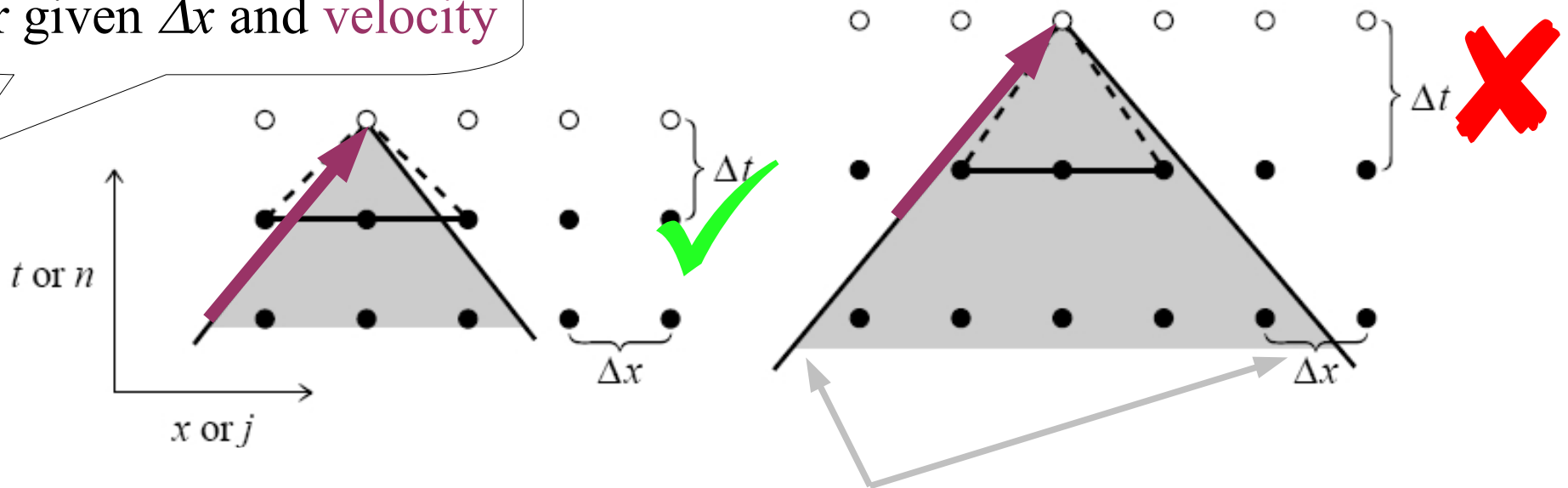
Courant-Friedrichs-Levy condition (CFL condition):

The numerical domain of dependence must contain the physical domain of dependence.

The CFL condition is necessary for stability, but not sufficient.

Domain of Dependence and CFL Condition

CFL condition limits Δt for given Δx and **velocity**



Hyperbolic PDEs have a finite physical domain of dependence due to the finite travelling speed of waves (\leftrightarrow characteristics).

Example: linear advection equation

$$|u\Delta t / \Delta x| \leq 1$$

constant flow velocity (everywhere, at all times) \rightarrow

characteristics = straight lines, slope corresponding to velocity

physical domain of dependence = starting point of characteristic

Truncation Error

A sufficiently smooth function can be expanded in a Taylor series:

$$\rho(x + \Delta x, t) = \sum_{l=0}^{\infty} \frac{1}{l!} \left. \frac{\partial^l \rho}{\partial x^l} \right|_{x,t} \Delta x^l = \rho(x, t) + \left. \frac{\partial \rho}{\partial x} \right|_{x,t} \Delta x + O(\Delta x^2) .$$

Solving for $\frac{\partial \rho}{\partial x}$ gives

$$\frac{\partial \rho}{\partial x} = \frac{\rho(x + \Delta x, t) - \rho(x, t)}{\Delta x} + O(\Delta x) .$$

Repeating this for the time derivative and applying it to an entire PDE (FTFS) gives

$$\underbrace{\frac{\partial \rho}{\partial t} + v \frac{\partial \rho}{\partial x}}_{\text{PDE}} = \underbrace{\frac{\rho_i^{n+1} - \rho_i^n}{\Delta t} + v \frac{\rho_{i+1}^n - \rho_i^n}{\Delta x}}_{\text{numerical scheme}} + \underbrace{O(\Delta t, \Delta x)}_{\text{truncation error}} .$$

The order of the truncation error is $O(\Delta t, \Delta x)$ in this case (FTFS).

A high order of the truncation error hints at good accuracy for smooth functions.

Consistency – Stability – Convergence

Consistency: A numerical scheme is consistent if its discrete operator (with finite differences) converges towards the continuous operator (with derivatives) of the PDE for $\Delta t, \Delta x \rightarrow 0$ (vanishing truncation error).

Stability: “Noise” (from initial conditions, round-off errors, ...) does not grow.

Convergence: The solution of the numerical scheme converges towards the real solution of the PDE for $\Delta t, \Delta x \rightarrow 0$

Lax's equivalence theorem: “Given a properly posed initial value problem and a finite difference approximation to it that satisfies the consistency condition, stability is the necessary and sufficient condition for convergence.”

Introduction to Numerical Hydrodynamics

2. The Linear Advection Equation



2.4 Examples of Numerical Schemes

Parameters of the Following Examples

Boundary conditions influence the properties of real world hydrodynamic flows.

Linear 1D advection: infinite domain without boundaries

Actual implementation of boundary conditions in numerical experiments: adding **ghost cells**, number depends on stencil.

In the following examples: **periodic boundary conditions**

$$v\Delta t / \Delta x = 0.4 \text{ (Courant Number)}$$

200 grid points

500 time steps

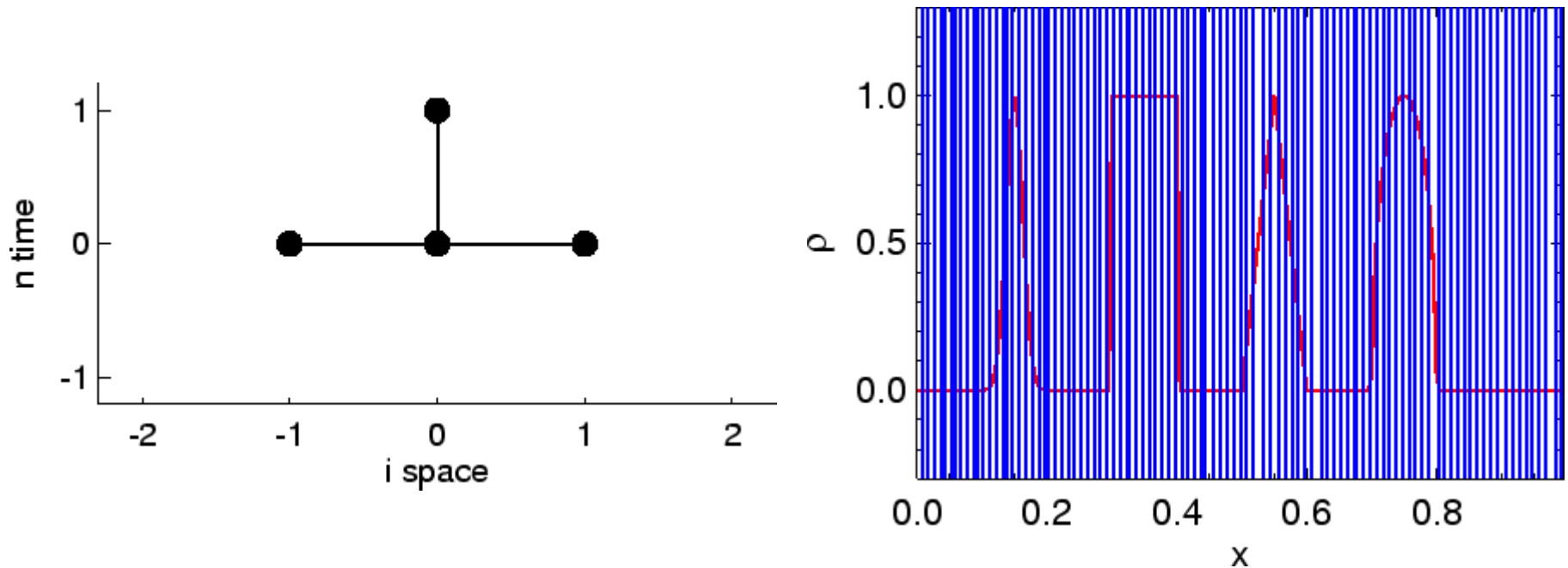
⇒ one full cycle

update formula:

$$\rho_i^{n+1} = \rho_i^n - \frac{\Delta t}{\Delta x} \left(f_{i+\frac{1}{2}}^n - f_{i-\frac{1}{2}}^n \right)$$

Initial condition: “spikes” (Gaussian, rectangle, triangle, half-ellipse), see Jiang & Shu (1996)

Linear Advection – Naïve FTCS Scheme



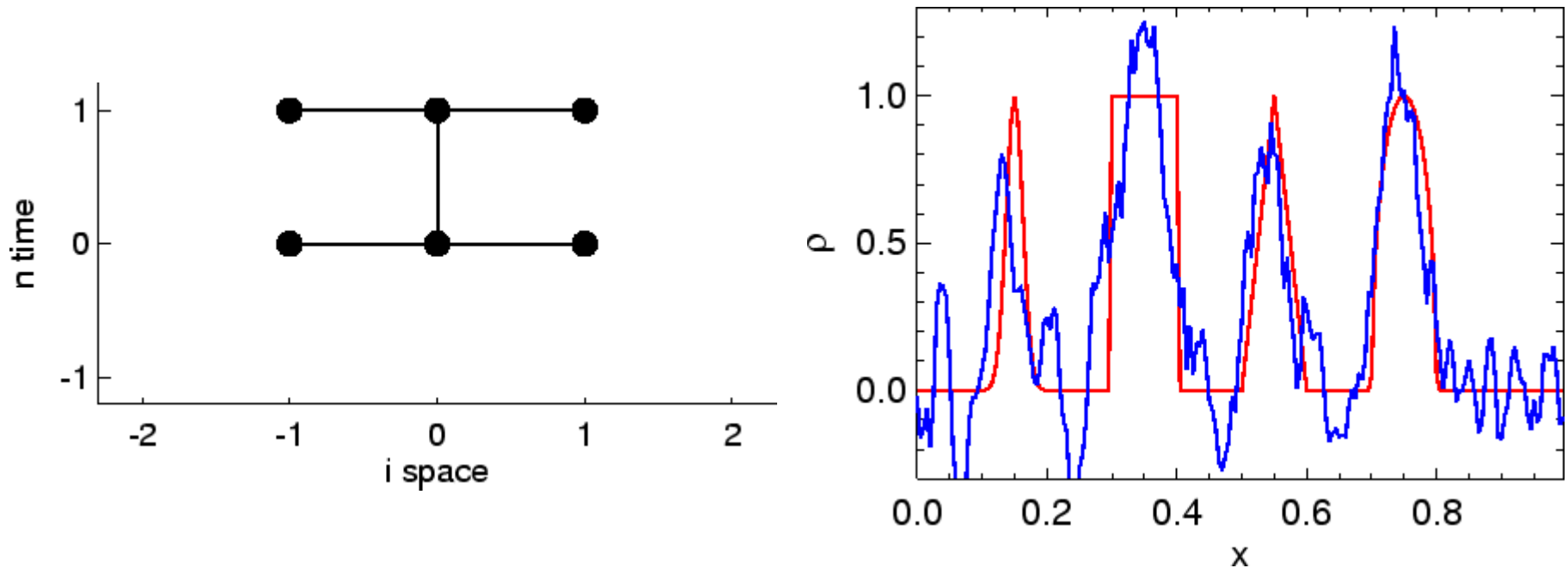
Figures courtesy of Bernd Freytag

Stencil diagram and (disastrous) test result (initial condition: red, solution: blue) for explicit Euler scheme (FTCS) with flux at $i + \frac{1}{2}$

$$f_{i+\frac{1}{2}}^n = \frac{1}{2} [f(\rho_{i+1}^n) + f(\rho_i^n)] .$$

The oscillations already seen earlier grow exponentially. After some time the numerical result does not have the faintest resemblance with the true solution.

Linear Advection – Implicit Centered Scheme



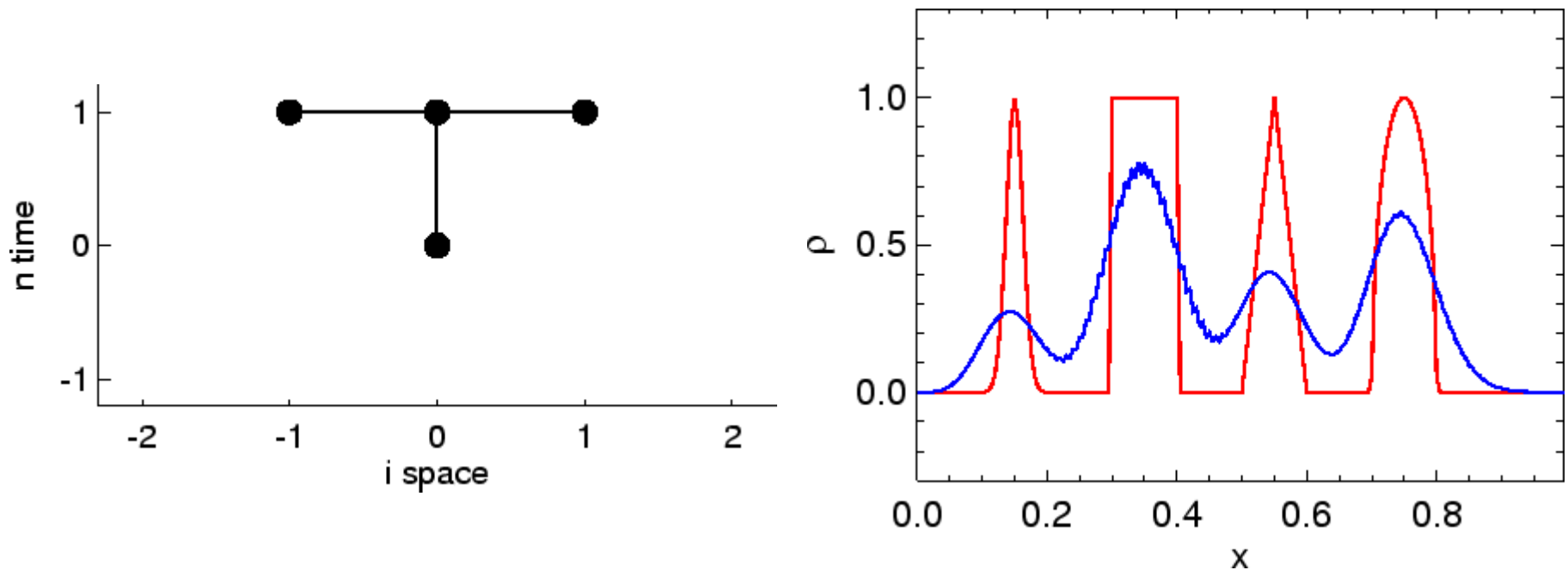
Figures courtesy of Bernd Freytag

Stencil diagram and test result (initial condition: red, solution: blue) for implicit centered scheme with flux

$$f_{i+\frac{1}{2}}^n = \frac{1}{4} [f(\rho_{i+1}^n) + f(\rho_i^n)] + \frac{1}{4} [f(\rho_{i+1}^{n+1}) + f(\rho_i^{n+1})] .$$

The centering of the scheme in space and time seems promising. However, the initial conditions is severely distorted.

Linear Advection – BTCS Scheme



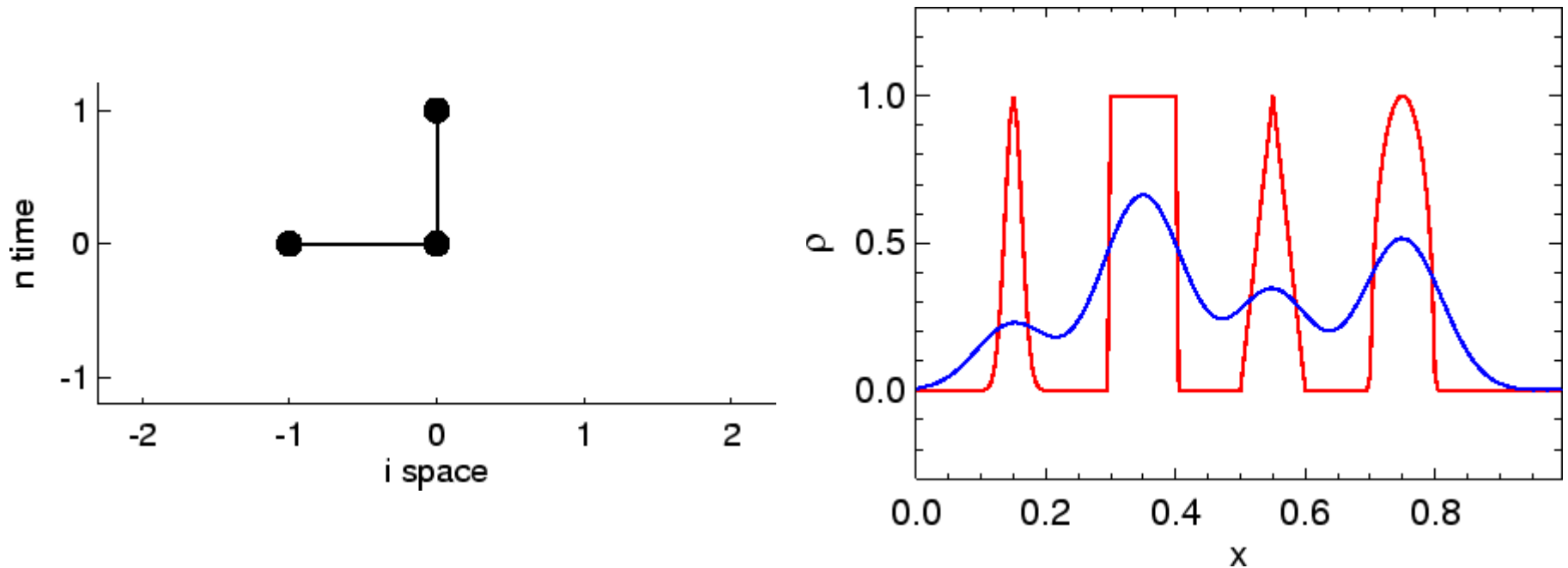
Figures courtesy of Bernd Freytag

Stencil diagram and test result (initial condition: red, solution: blue) for fully implicit BTCS scheme with flux

$$f_{i+\frac{1}{2}}^n = \frac{1}{2} [f(\rho_{i+1}^{n+1}) + f(\rho_i^{n+1})] .$$

The fully implicit treatment takes effect: the result looks almost smooth (with some non-decaying small-scale wiggles) but is smeared out heavily.

Linear Advection – Donor Cell (FTBS) Scheme



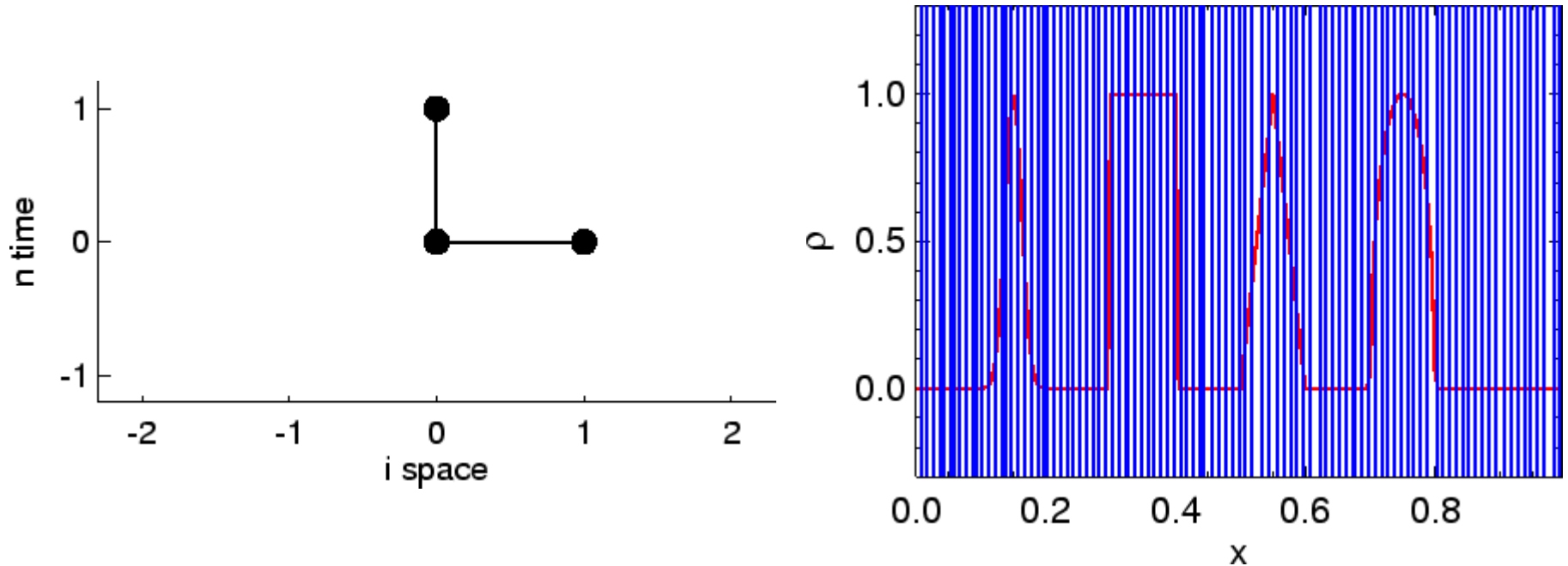
Figures courtesy of Bernd Freytag

Stencil diagram and test result (initial condition: red, solution: blue) for donor cell (FTBS) scheme with flux

$$f_{i+\frac{1}{2}}^n = f(\rho_i^n) \quad .$$

The result is wonderfully smooth but smeared out severely. Upwinding seems promising to achieve stability. However, the accuracy of the scheme has to be improved.

Linear Advection – FTFS Scheme



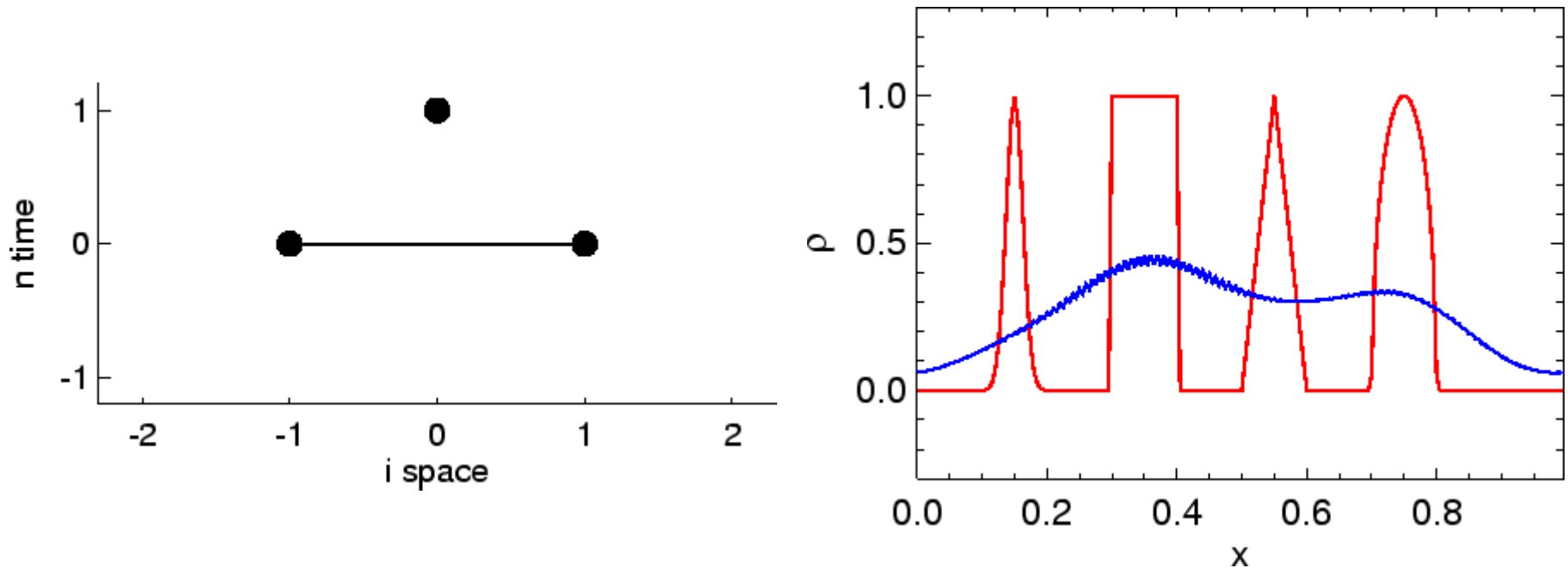
Figures courtesy of Bernd Freytag

Stencil diagram and (disastrous) test result (initial condition: red, solution: blue) for FTFS scheme with flux

$$f_{i+\frac{1}{2}}^n = f(\rho_{i+1}^n) .$$

Small-scale oscillations grow even faster than for the naïve scheme and render the FTFS scheme useless (for $v > 0$).

Linear Advection – Lax-Friedrichs Scheme



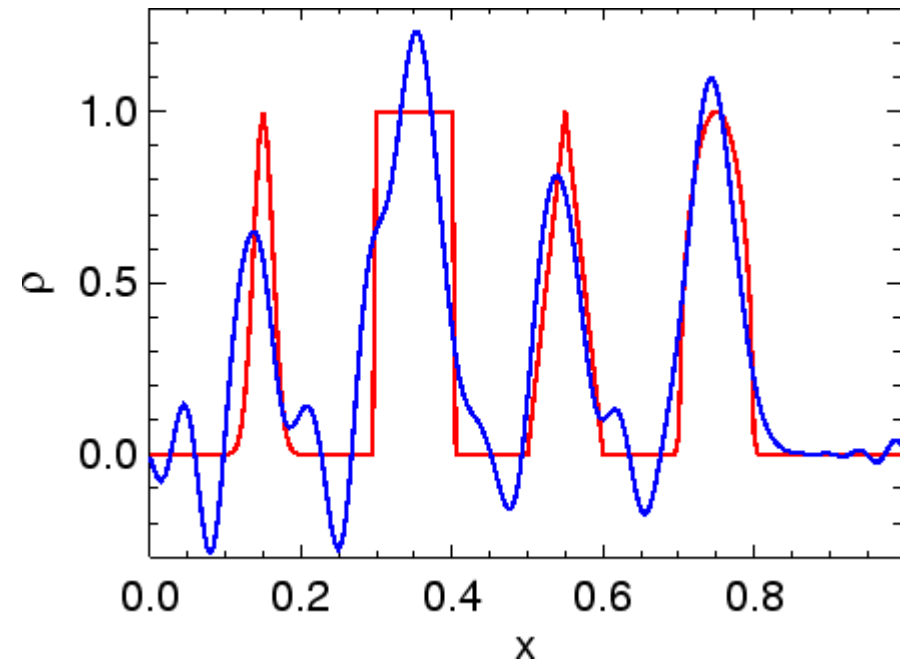
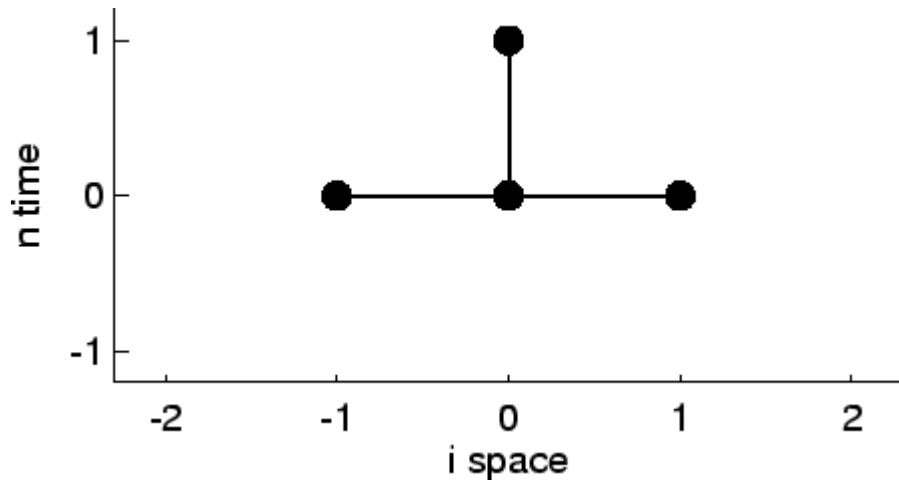
Figures courtesy of Bernd Freytag

Stencil diagram and test result (initial condition: red, solution: blue) for Lax-Friedrichs scheme with flux

$$f_{i+\frac{1}{2}}^n = \frac{1}{2} [f(\rho_{i+1}^n) + f(\rho_i^n)] - \frac{1}{2} \frac{\Delta x}{\Delta t} [\rho_{i+1}^n - \rho_i^n] .$$

The smearing is so strong that not even the number of initial spikes is conserved. And there are some non-decaying small-scale wiggles left. Note: odd-even decoupling.

Linear Advection – Lax-Wendroff Scheme



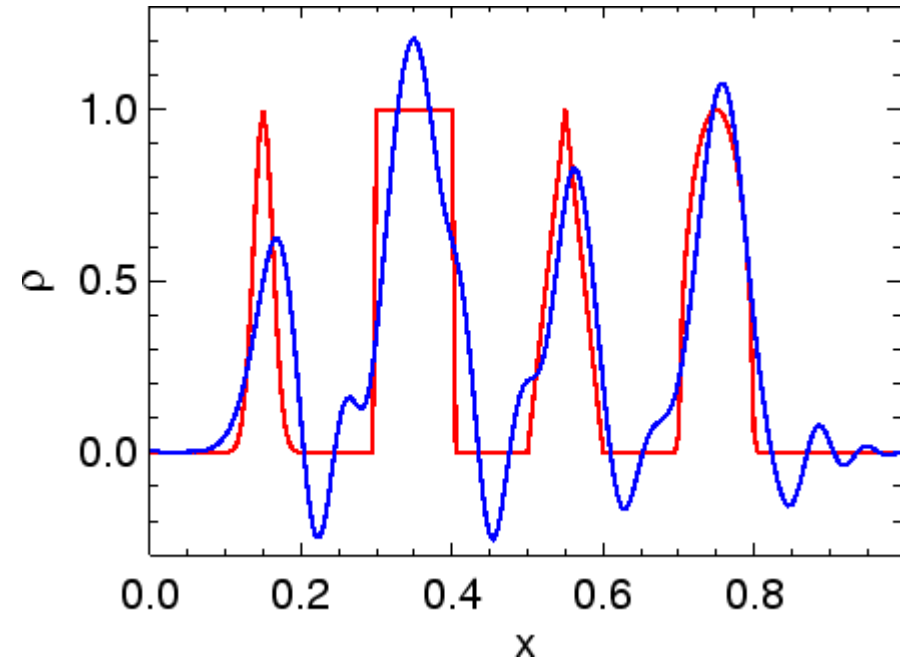
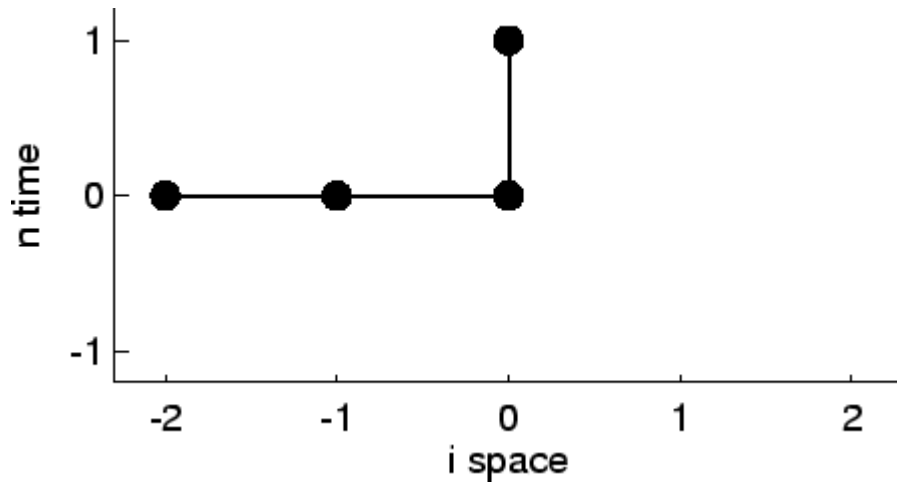
Figures courtesy of Bernd Freytag

Stencil diagram and test result (initial condition: red, solution: blue) for Lax-Wendroff scheme ($O(\Delta x^2, \Delta t^2)$) with flux

$$f_{i+\frac{1}{2}}^n = \frac{1}{2} [f(\rho_{i+1}^n) + f(\rho_i^n)] - \frac{1}{2} \frac{v^2 \Delta t}{\Delta x} [\rho_{i+1}^n - \rho_i^n] .$$

The result is smooth with considerable overshoot (that does not grow much with time any more). This second order scheme might be useful for more regular initial conditions.

Linear Advection – Beam-Warming Scheme



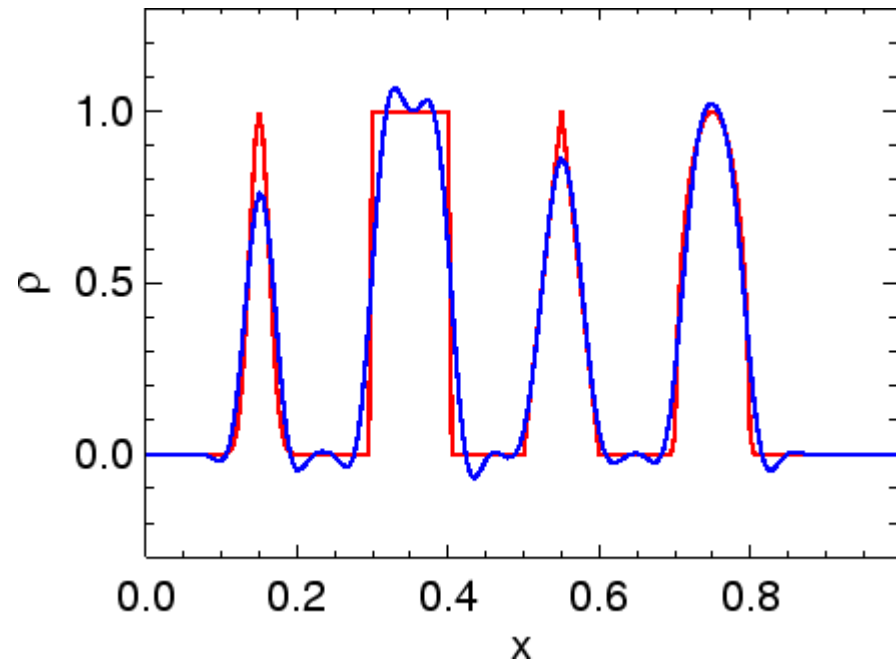
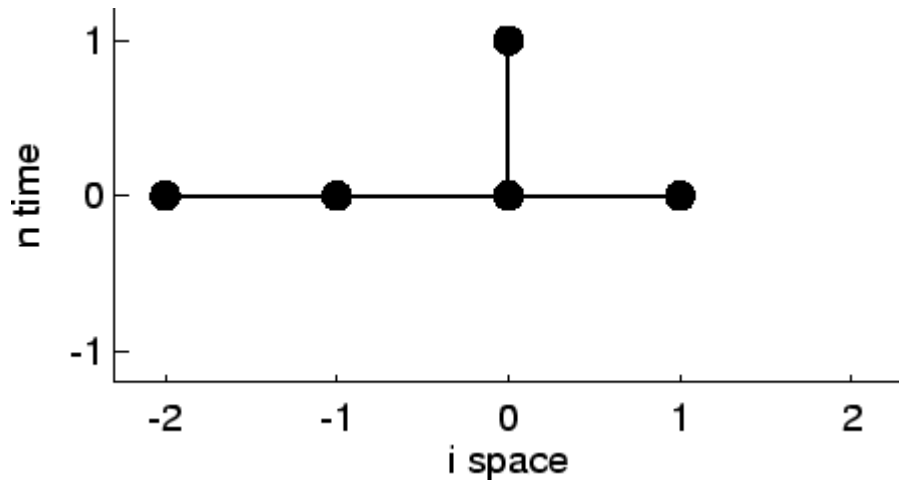
Figures courtesy of Bernd Freytag

Stencil diagram and test result (initial condition: red, solution: blue) for Beam-Warming scheme ($O(\Delta x^2, \Delta t^2)$) with flux

$$f_{i+\frac{1}{2}}^n = \frac{1}{2} [3f(\rho_i^n) - f(\rho_{i-1}^n)] - \frac{1}{2} \frac{v^2 \Delta t}{\Delta x} [\rho_i^n - \rho_{i-1}^n] \quad .$$

The result is smooth with considerable overshoot (that does not grow much with time any more). This second order scheme might be useful for more regular initial conditions.

Linear Advection – Fromm Scheme



Figures courtesy of Bernd Freytag

Stencil diagram and test result (initial condition: red, solution: blue) for Fromm scheme ($O(\Delta x^2, \Delta t^2)$) with flux

$$f_{i+\frac{1}{2}}^n = \frac{1}{2} \left(f_{\text{Lax-Wendroff}, i+\frac{1}{2}}^n + f_{\text{Beam-Warming}, i+\frac{1}{2}}^n \right) .$$

The result is smooth with some amount of overshoot. The initial shape of the spikes is recognizable. So far the best scheme, if the overshoot can be accepted.

The Linear Advection Equation – Homework 2

Compute the numerical solution of the linear advection equation

$$\frac{\partial \rho}{\partial t} + u \frac{\partial \rho}{\partial x} = 0$$

in the range $0 \leq x \leq 1$, with the initial conditions

$$\rho_0(x) = 1 \quad \text{for } x < 0 \quad \text{and} \quad \rho_0(x) = 0 \quad \text{for } x > 0$$

assuming $u=1$ and $\Delta t/\Delta x = 0.5$, for different numerical schemes:
(a) Lax-Friedrichs, (b) Lax-Wendroff and (c) Beam-Warming.

Plot the resulting numerical solutions and the exact analytical solution at time $t = 0.5$ for the cases $\Delta x = 0.01$ and $\Delta x = 0.0025$, and compare the results to the upwind (donor cell) scheme (see homework 1).